Article

Preparation and Characterization of Avermectin B2 Microcapsules and Effective Control of Root-Knot Nematodes

Liying Wang,* Xinxin Yan, Yan Li, Chong Gao, and Junzhi Liu
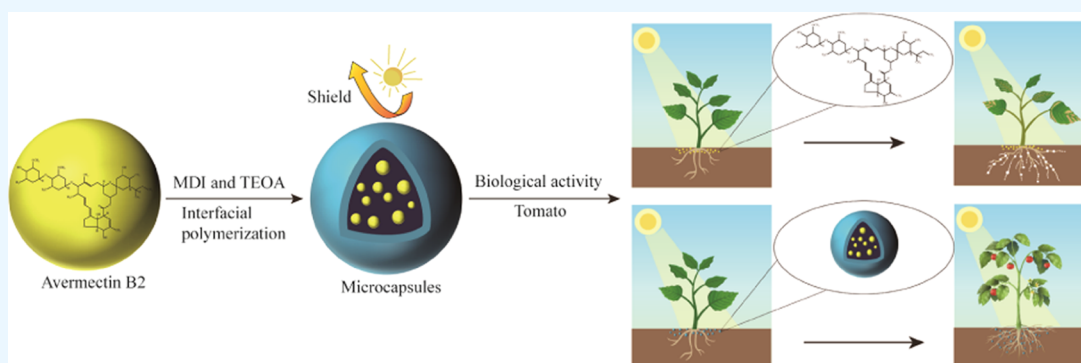
Read Online

ACCESS | 📊 Metrics & More | 📰 Article Recommendations

ABSTRACT: Polyurethane microcapsules of avermectin B2 were prepared by means of interfacial polymerization with methylene diphenyl diisocyanate as the wall material and triethanolamine as the initiator. The microcapsules were characterized by scanning electron microscopy, Fourier transform infrared spectroscopy, and thermogravimetric analysis. The surfaces of the microcapsules were found to be smooth and almost spherical, and the encapsulation efficiency was high. The avermectin B2 microcapsules exhibited a good diffusion-controlled sustained-release performance, giving a cumulative release rate of 91.81%. The results indicated that the polyurethane capsule protected against the photolysis of avermectin B2. Finally, the microcapsules exhibited good soil leaching properties and were able to control the population of root-knot nematodes with an efficacy of 80.80%.

1. INTRODUCTION

Root-knot nematodes are sedentary, soil-dwelling parasites that infect plant roots and disturb their nutrient and water uptake, ultimately leading to significant yield losses.[1] Indeed, it has been reported that root-knot nematode disease causes an annual loss of over $1 billion to the global economy.[2] According to statistics, approximately 30% of greenhouse vegetables worldwide are infected annually by root-knot nematodes, resulting in yield losses of 20−40%, and in many cases, a lack of harvest.[3−5] To address this issue, avermectin is commonly employed. Avermectin is a sixteen-membered macrolide insecticide extracted from the MA-4680 strain of Streptomyces avermitilis that can be isolated from the soil. A number of avermectin derivatives exist, namely, A1a, A2a, A1b, A2b, B1a, B2a, B1b, and B2b,[6−8] wherein avermectin B2 is known to exhibit a strong nematocidal activity.[9,10] Although this compound has been widely used to control crop diseases caused by infectious nematodes (e.g., root-knot nematodes, root rot nematodes, cyst nematodes, and stem nematodes),[11,12] it is susceptible to photolysis and a has poor mobility in the soil, thereby hindering its uptake by plants and lowering its potential efficacy.[13] However, despite the fact that various avermectin B2 preparations are available on the market, such as

emulsifiable concentrate (EC), microemulsion (ME), and emulsion in water (EW),[14,15] they are unable to solve the above issues. The development of microencapsulated formulations of avermectin B2 is therefore of interest to improve its anti-photolytic stability and soil migration rate to enhance its efficacy and extend its shelf life.

Pesticide microcapsules tend to employ natural, seminatural, or synthetic polymer materials to encapsulate active pesticide components as tiny particles by means of physical, chemical, and physical and chemical methods; this technology has been shown to achieve controlled release of the encapsulated pesticides.[16,17] To date, various methods have been reported for the preparation of microcapsules, including in situ polymerization, interfacial polymerization, emulsion polymerization, and solvent evaporation, among others.[18−24] Interfacial

polymerization is one of the most common methods used to produce pesticide microcapsules,[25] wherein the microcapsules are synthesized at the interface between the two phases. For example, interfacial polymerization has become the main method for microcapsule preparation in the field of pesticides because of its rapid encapsulation reaction, mild reaction conditions, and low degree of penetrability.[26,27] In this context, the main-chain polymer polyurethane (PU) exhibits attractive mechanical and chemical properties, in addition to presenting a good environmental safety profile.[28,29] As a result, PU has been widely used in various fields, and with regard to this work, PU is expected to improve pesticide stability, prolong its validity period, and reduce the toxicity of the pesticide to humans, animals, and environmental organisms. It would therefore be expected that the encapsulation of pesticides by PU could ultimately expand the application scope of these compounds.

Thus, we herein report the preparation of avermectin B2 microcapsules with a smooth surface and a high encapsulation efficiency through the interfacial polymerization of methylene diphenyl diisocyanate (MDI) as the wall material and triethanolamine (TEOA) as the initiator. Subsequently, the controlled release behavior, anti-photolysis stability, and soil mobility of the prepared avermectin B2 microcapsules are systematically studied, as is their ability to control the population of root-knot nematodes.

2. RESULTS AND DISCUSSION

2.1. Effect of the MDI Addition Amount on Microcapsule Preparation.
The microcapsules were synthesized by means of interfacial polymerization. During this process, the amount of emulsifier, the preparation temperature, the stirrer speed during emulsion preparation, and the core/shell ratio influence the physicochemical properties of the resulting microcapsules. For example, the core/shell ratio has been reported to affect the particle size, encapsulation efficiency, and release behavior.[30] Thus, we initially investigated the effects of the MDI addition amount on the final particle size and encapsulation efficiency.

As shown in Table 1, upon increasing the MDI addition amount from 2.5 to 7.5 g, the D_{50} value increased from 2.58 to

Table 1. Effects of Different MDI Addition Amounts on the Microcapsule Particle Size Distribution and Encapsulation Efficiency

sample	wall material (g)	size distribution (μm)			EE (%)
		D_{10}	D_{50}	D_{90}	
1	2.5	1.15	2.58	5.38	81.73
2	5.0	1.72	4.22	7.53	90.21
3	7.5	3.42	9.84	18.40	91.82

9.84 μm, and the EE increased from 81.73 to 91.82%. These results indicate that an increased MDI addition amount affected both the particle size and the encapsulation rate. It should be noted that when the MDI addition amount was 5.0 or 7.5 g, the encapsulation rate was >90%; however, the average particle size was smaller when 5.0 g MDI addition amount was employed. At a constant drug mass, increasing the amount of MDI addition amount increased the thickness of the capsule shell and increased the particle size, which resulted in a relatively slow release of avermectin B2. Thus, considering the average particle size and encapsulation rate, an MDI addition amount of 5.0 g was selected as the optimal content.

2.2. Characterization of the Avermectin B2 Microcapsules.
2.2.1. Morphological Characteristics and Particle Size Distributions of the Microcapsules. Figure 1A shows an SEM image of the avermectin B2 microcapsules, which can be seen to exhibit a regular spherical shape with a smooth and dense surface and a uniform particle size. In agreement with the results reported by Zhao et al.,[31] the MDI-encapsulated microcapsules possessed an ideal spherical shape. In addition, Figure 1B shows the particle size distribution of the avermectin B2 microcapsules. A normal-shaped particle size curve can be seen, in addition to a relatively narrow particle size distribution, as evidenced by a D_{50} value of 4.04 μm and a particle span of 1.45. It should be noted that the particle span represents the width of the particle size distribution, wherein a smaller value indicates a more uniform particle size and a greater size consistency.

2.2.2. FTIR Spectroscopy of the Microcapsules. Figure 2 shows the FTIR spectra of the technical avermectin B2, the prepared avermectin B2 microcapsules, and the blank microcapsules. More specifically, in the FTIR spectrum of the technical avermectin B2 (Figure 2A), the broad peaks at 3000−2850 cm^{-1} originated from the−CH$_3$ and −CH$_2$ stretching vibrations, while the sharp absorption peak at 1720 cm^{-1} was attributed to the −C═O stretching vibration.

In addition, in the FTIR spectrum of the blank microcapsules (Figure 2C), the three absorption peaks observed between 1600 and 1450 cm^{-1} originated from vibrations of the benzene ring skeleton, while the broad peak at 2250 cm^{-1} belonged to the stretching vibration of the N═C═O bond in the isocyanate group. Compared with the spectrum recorded for the blank microcapsules, the absorption peak of the isocyanate group in the avermectin B2 microcapsules (Figure 2B) was significantly diminished. Furthermore, a strong absorption peak corresponding to the C−O stretching vibration appeared at 1250 cm^{-1}. These results indicate that the successful reaction between MDI and TEOA converted the N═C═O group into a N−C═O group and an ester bond was also formed; similar results were reported by Zheng et al.[32] Moreover, the methyl and methylene absorption peaks were significantly less intense in the spectrum of the avermectin B2 microcapsules than for the technical avermectin B2 microcapsule sample, indicating that avermectin B2 had been successfully encapsulated by the capsule wall generated upon the reaction of MDI with TEOA.

2.2.3. Thermal Analysis of the Microcapsules. The TGA weight loss curves of the blank microcapsules, the avermectin B2 microcapsules, and the technical avermectin B2 are shown in Figure 3 (curves A−C, respectively). As can be seen from curve A, the weight loss exhibited by the capsule material could be roughly divided into two stages, namely, decomposition of the polyurethane capsule below 450 °C, followed by the continuous decomposition of its residue beyond this point. In addition, from curve C, it can be seen that the weight loss of the active avermectin B2 could also be divided into two stages. In this case, the first stage involved decomposition of the active drug (<270 °C), corresponding to a weight loss of 75.44%, while the second stage constituted residue decomposition at higher temperatures, corresponding to a weight loss of 22.43%; the weight loss rate of the latter stage was significantly lower than that of the former stage. Thus, from curve B, it was deduced that the weight loss process of the avermectin B2 microcapsules initially involved microcapsule decomposition prior to a more rapid decomposition of the avermectin B2 drug
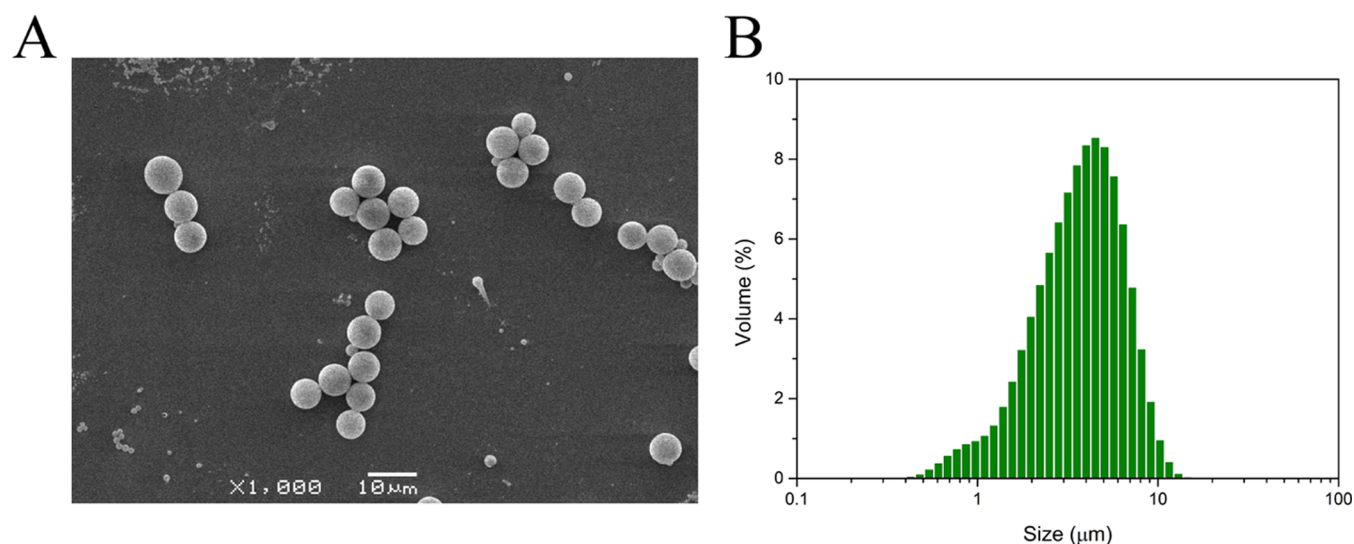
Figure 1. (A) SEM image of the avermectin B2 microcapsules. (B) Particle size distribution of the avermectin B2 microcapsules.
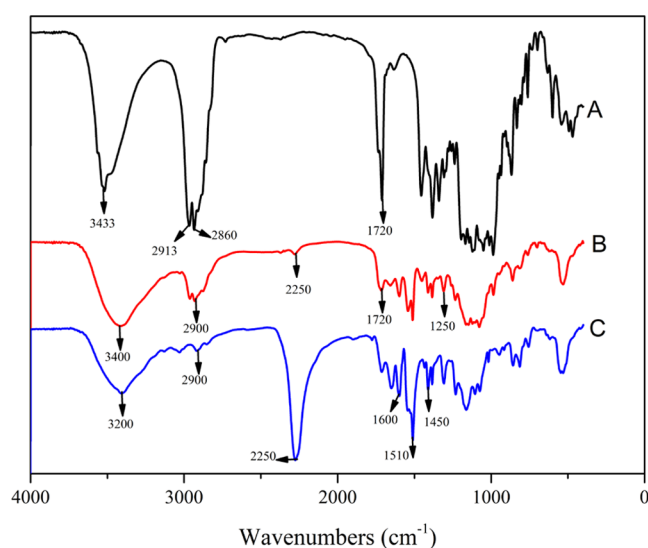

Figure 2. FTIR spectra of (A) the technical avermectin B2, (B) the avermectin B2 microcapsules, and (C) the blank microcapsules.
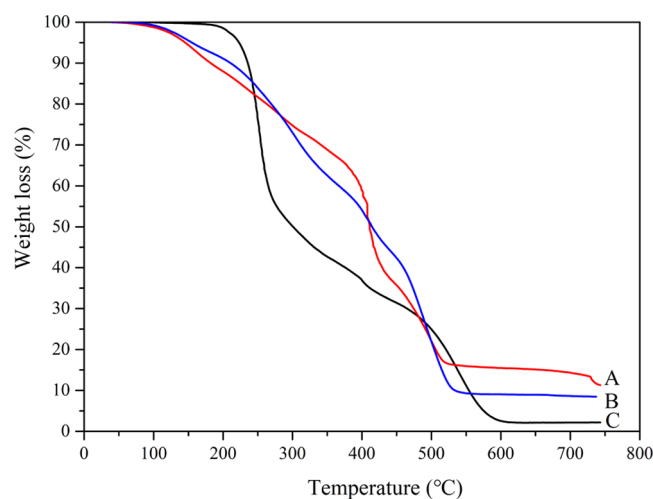

Figure 3. TGA weight loss curves of (A) the blank microcapsules, (B) the avermectin B2 microcapsules, and (C) the technical avermectin B2.
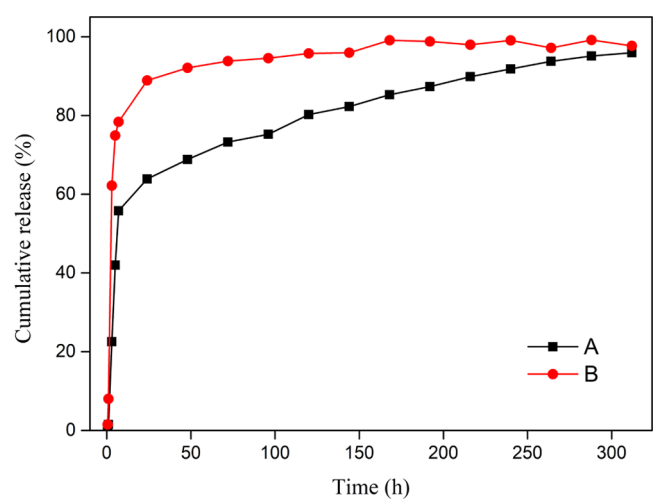
Figure 4. Comparison of avermectin B2 release from different formulations. (A) Avermectin B2 microcapsules and (B) the commercial avermectin B2 EC.

molecules, thereby confirming the successful coating of avermectin B2 with the isocyanate material, and demonstrating the good thermal stability of the prepared microcapsules.

2.3. Release Behavior and Kinetics of the Microcapsules. *2.3.1. Comparison of Sustained Release between the Microcapsules and Commercial Formulations.* The release behaviors of the prepared avermectin B2 microcapsules and the commercial avermectin B2 EC were investigated, as presented in Figure 4. In the case of the commercial specimen (curve B), an initial rapid release was observed within 5 h (i.e., 74.93%), with complete release taking place by 48 h. In contrast, avermectin B2 was released more slowly from the microcapsules (curve A), with a release of 41.98% being reached at 5 h, followed by a slow and sustained release to a cumulative release of 91.81% after 240 h. These results indicate that under the same conditions, the avermectin B2 microcapsules exhibited a longer sustained-release profile than the commercial avermectin B2 EC, thereby confirming the ability of our system to exhibit a sustained release. Indeed, it should be noted that Fu et al.[33] previously reported that avermectin

polyurea microcapsules prepared from chitosan oligomers and MDI exhibited a long (120 h) sustained-release performance, thereby confirming the potential of such systems.

2.3.2. Effect of pH on the Avermectin B2 Release Rate from the Microcapsules.

Since avermectin B2 is used as a root irrigation treatment to control nematodes, the soil environment must be considered due to its potential role in influencing the efficacy of the formulation. Thus, the effects of different pH levels on the release of avermectin B2 from the microcapsules were evaluated, as shown in Figure 5. More
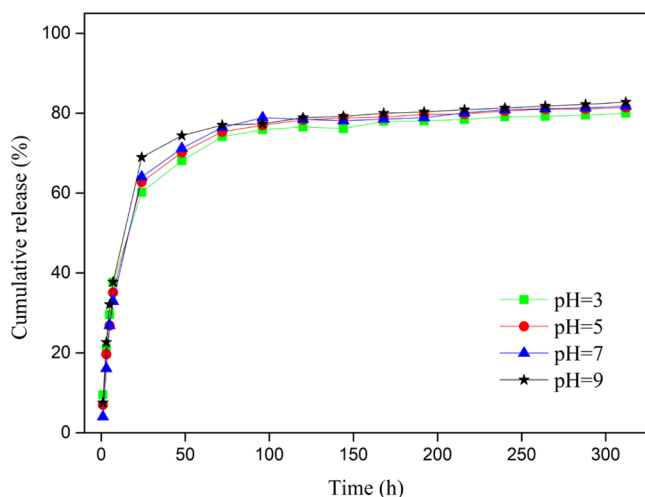
Figure 5. Effects of pH on the release of avermectin B2 from the prepared microcapsules.

specifically, at pH values of 3, 5, 7, and 9, the release of avermectin B2 showed a two-stage trend, with a significant release (60%) being observed in the initial stage (within 24 h), followed by a continuous and slow release (cumulative release >80%) with no significant differences in release trends between pH conditions. These results therefore indicate that the prepared avermectin B2 microcapsules can be applied in soils with different pH values, thereby rendering them potentially suitable for future applications in both acidic and alkaline soils.

Subsequently, the zero-order, first-order, Higuchi, and Ritger–Peppas models were used to investigate the kinetics of avermectin B2 release from the microcapsules at different pH values, and the associated correlation coefficients (R^2) were constructed to assess the release mechanism under each set of conditions. As presented in Table 2, the release of avermectin B2 from the microcapsules under the various pH conditions examined herein fit best with the first-order model ($R^2 >$ 0.978), and in all cases, simple diffusion appeared to dominate, with an exponentially decreasing release rate over time.

2.4. Photodegradation Experiments.
Avermectin B2 is known to be susceptible to photodegradation when exposed to natural light, and as a result, the degradation of avermectin B2

deposited on a soil surface can reduce its effectiveness. Therefore, anti-photodegradation formulations are necessary to reduce the breakdown of avermectin B2 and improve its efficiency. Figure 6 shows the stabilities of the avermectin B2

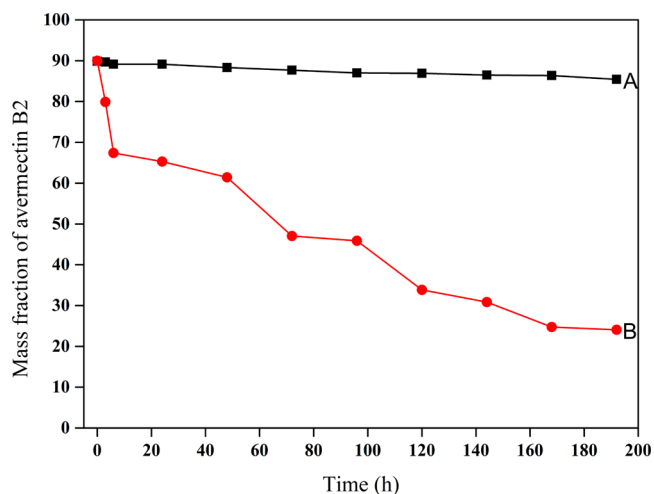**Figure 6.** Stabilities of (A) the avermectin B2 encapsulated in the prepared microcapsules and (B) the technical avermectin B2 under natural light.

microcapsules (curve A) and the technical avermectin B2 (curve B) under natural light. As shown, the technical avermectin B2 degraded by 53.8% within 100 h, while the avermectin B2 present in the prepared microcapsules degraded by only 3.33% within the same time. In addition, after 192 h, the technical avermectin B2 had degraded by 65.95%, whereas the encapsulated avermectin B2 had degraded by <4.43%. It is therefore apparent that the encapsulation process delays the degradation of avermectin B2 by >15 times, and so the polyurethane shell can be considered to possess photo-degradation-shielding properties.

2.5. Soil Leaching Test.
The rate of pesticide movement in a soil specimen is influenced by the nature of the pesticide (e.g., its adsorption and degradation properties) and the field conditions (e.g., the soil properties), wherein the nature of the pesticide plays a key role.[34,35] Although avermectin B2 has been shown to exhibit a good biological activity against nematodes, it is not effective in controlling nematodes in practical applications.

More specifically, due to the poor mobility of avermectin B2 in the soil, it is difficult to provide widespread protection of the plant roots, and the potential for nematode damage is significant. Indeed, this was confirmed herein using a soil column drenching test, wherein Avermectin B2 was not detected in the leaching solutions of either formulation. As shown in Figure 7, the detected concentrations of avermectin B2 in the microcapsule suspension (CS) and in the

Table 2. Fitting Parameters for the Avermectin B2 Release Profiles Using Different Kinetic Models

| pH	Zero order		First order		Higuchi model		Ritger–Peppas model	
	equation	R^2	equation	R^2	equation	R^2	equation	R^2
3	$Q_t = 42.271 + 0.165t$	0.548	$Q_t = 76.746(1 - \exp(-0.088t))$	0.978	$Q_t = 3.599 + 27.906t^{1/2}$	0.762	$Q_t = 24.592t^{0.221}$	0.885
5	$Q_t = 1.745 + 0.174t$	0.536	$Q_t = 78.627(1 - \exp(-0.078t))$	0.988	$Q_t = 3.824 + 26.408t^{1/2}$	0.752	$Q_t = 23.643t^{0.232}$	0.871
7	$Q_t = 40.930 + 0.179t$	0.517	$Q_t = 79.075(1 - \exp(-0.073t))$	0.993	$Q_t = 3.941 + 25.012t^{1/2}$	0.732	$Q_t = 22.777t^{0.240}$	0.851
9	$Q_t = 44.800 + 0.165t$	0.502	$Q_t = 79.636(1 - \exp(-0.095t))$	0.991	$Q_t = 3.644 + 30.046t^{1/2}$	0.716	$Q_t = 26.386t^{0.214}$	0.850
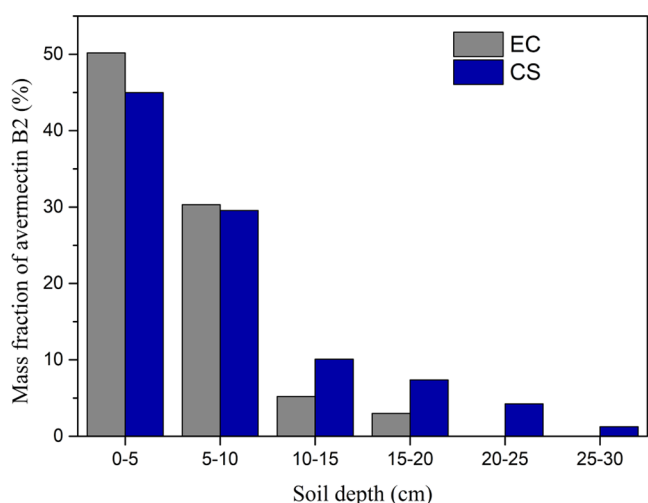
Figure 7. Leaching distributions of the commercial avermectin B2 emulsifiable concentrate and the avermectin B2 microcapsules from the soil columns.

commercially available avermectin B2 emulsifiable concentrate (EC) gradually decreased in the soil samples as the depth increased. More specifically, at a soil depth of 20−25 cm, the commercial avermectin B2 emulsion was not detected, although the microcapsule suspension was detected (4.25%). At an increased depth of 25−30 cm, the microcapsule suspension was still detected (1.26%), thereby confirming its good mobility in the soil. These results provide a good basis for controlling root-knot nematodes.

2.6. Bioactivity Determination for the Avermectin B2 Microcapsule Suspension in the Laboratory. To verify the feasibility of developing an avermectin B2 microcapsule suspension as a new pesticide formulation, trials were conducted using the potted root irrigation method to control the second instar larvae of the root-knot nematodes in cucumber seedlings. Figure 8 shows the effects imparted by the technical avermectin B2, avermectin B2 microcapsules, and the treatment-free incubation specimen over a period of 15 d.

As shown, the avermectin B2 microcapsule suspension was significantly more effective than avermectin B2 alone in controlling root-knot nematodes. Table 3 shows the analytical model for the toxicities of the technical avermectin B2 and the prepared avermectin B2 microcapsules. As indicated, the EC_{50} values for these species were 1.93 and 1.28 mg/L, respectively, and these results are consistent with the in-pot experiments. It was therefore clear that the efficacy of avermectin B2 clearly increased after encapsulation with polyurethane.

2.7. Field Efficacy Experiment Using the Avermectin B2 Microcapsule Suspension. The application performance of avermectin B2 microcapsules were verified by means of field efficacy trials, and the results were compared with those obtained for the technical avermectin B2 EC. Thus, the symptoms of a 60 d root-knot nematode infection in the plant root system can be seen in Figure 9, wherein it is apparent that the degree of root damage was reduced in the treatment groups after this time. In contrast, the untreated roots were severely infected and exhibited the most severe root swelling. Table 4 outlines the experimental results obtained during root-knot nematode control by the avermectin B2 microcapsules and by the technical avermectin B2 EC. More specifically, at loadings of 225 and 375 g ai/hm², the average degrees of control achieved using the avermectin B2 microcapsules reached 71.69 and 80.80%, respectively, while lower corresponding values of 43.96 and 68.77% were obtained for the avermectin B2 EC specimen. These results confirm the superior control effect exhibited by the avermectin B2 microcapsules compared to the avermectin B2 EC at the same dosage. Moreover, similar results were obtained for an avermectin B2 microcapsule dosage of 225 g ai/hm² and an avermectin B2 EC dosage of 375 g ai/hm², thereby indicating the possibility of reducing the dosage while also improving the efficacy.

3. CONCLUSIONS

In this study, avermectin B2 microcapsules were prepared by means of an interfacial polymerization approach, wherein methylene diphenyl diisocyanate (MDI) was used as the wall material, and triethanolamine (TEOA) was employed as the
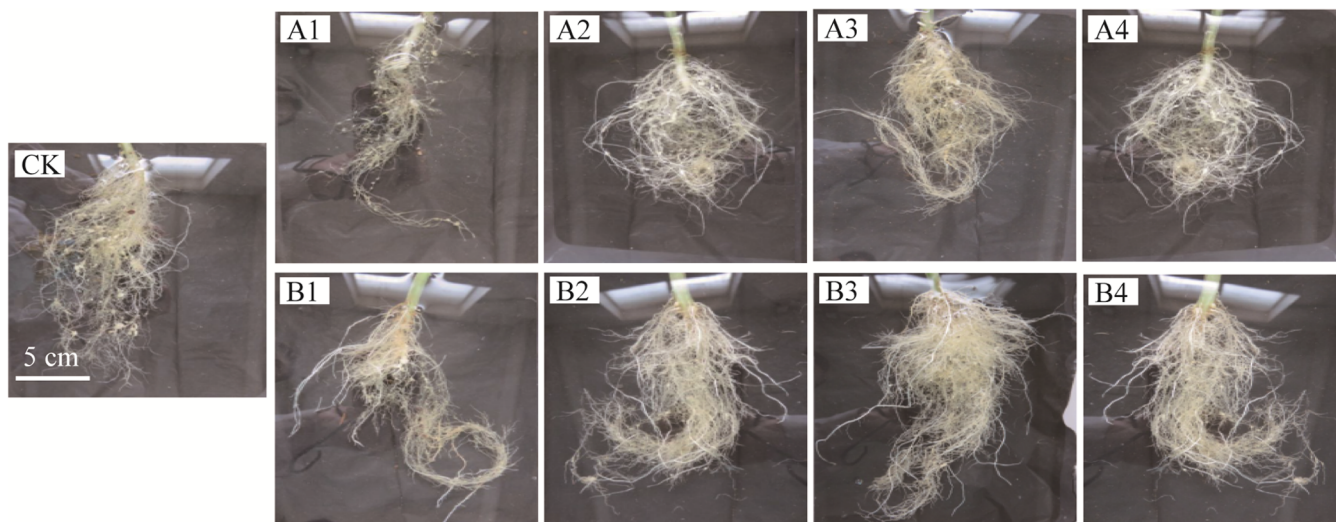

Figure 8. Photographic images of the cucumber roots infected with root-knot nematodes and the control effects of (A) the technical avermectin B2 and (B) the avermectin B2 microcapsules at concentrations of 0.625 mg/L (1), 1.25 mg/L (2), 2.5 mg/L (3), and 5 mg/L (4) on day 15 of treatment. A corresponding image is also shown for the control check (CK).

Table 3. Toxicity Analysis Models for Technical Avermectin B2 and its Formulations

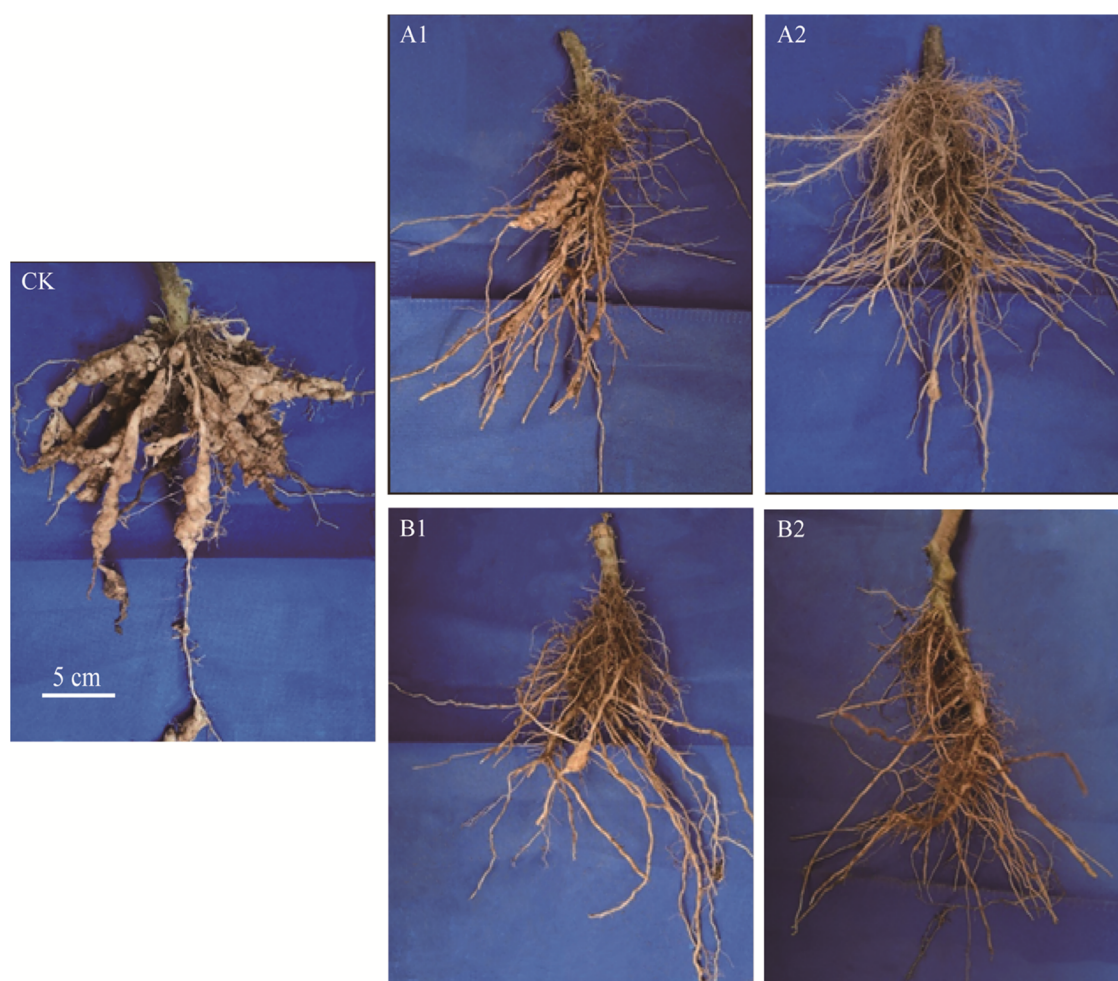| formulations	EC50 (mg/L)	regression equation	correlation coefficient	confidence interval
technical avermectin B2	1.93	$Y = 4.63 + 1.30X$	0.9997	1.8785−1.9747
avermectin B2 microcapsule suspension	1.28	$Y = 4.83 + 1.57X$	0.9978	1.1859−1.3820

Figure 9. Photographic images of the tomato roots infected with root-knot nematode and the control effects of (A) avermectin B2 EC and (B) the avermectin B2 microcapsules at concentrations of 225 g ai/hm^2 (1) and 375 g ai/hm^2 (2) on the 60th day of treatment. A corresponding image is also shown for the control check (CK).

Table 4. Effects of the Avermectin B2 Microcapsules on the Control of the Tomato Root-Knot Nematodes

formulations	dosage (g ai/hm^2)	effect of control (%)	significant difference 5%	significant difference 1%
avermectin B2 microcapsules	225	71.69	a	AB
	375	80.80	a	A
commercial avermectin B2 EC	225	43.96	b	AB
	375	68.77	ab	AB

initiator. The surfaces of the prepared microcapsules were found to be smooth, and they exhibited an average particle size of 4.04 μm and an encapsulation efficiency of >90%. Fourier transform infrared and thermogravimetric analyses confirmed that the avermectin B2 pesticide had been successfully encapsulated by the polymeric material. Subsequently, in

vitro release studies showed that the avermectin B2 microcapsules could consistently and optimally release the active drug at pH values ranging from 3 to 9, thereby indicating their potential for future applications in either acidic or alkaline soils. Furthermore, photodegradation studies showed that encapsulation was effective in improving the resistance of avermectin B2 to photolysis. Moreover, soil column leaching tests demonstrated that the prepared avermectin B2 microcapsules exhibited good mobility in the soil, and so these combined factors resulted in superior and extended protection of the root system. Indoor and field applications against nematodes showed that these avermectin B2 microcapsules were more effective than technical avermectin B2 and an avermectin B2 emulsified suspension. Finally, the avermectin B2 microcapsules described herein provide a new choice of dosage form for the market while also addressing the issues related to photodegradation and poor soil mobility, which are commonly associated with existing dosage forms. Overall, these results are of great significance for improving the field
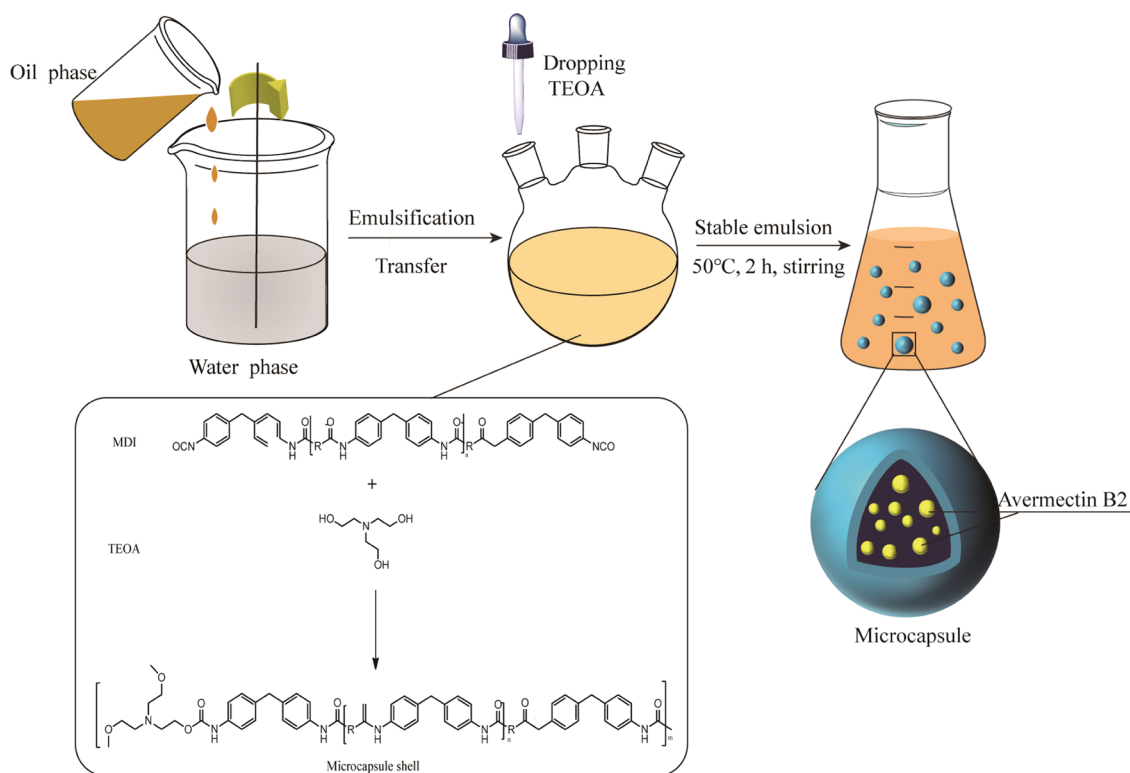
Figure 10. Outline of the preparation process employed to obtain the avermectin B2-containing microcapsules. The corresponding reaction for microcapsule formation is also shown.

control effect and application of avermectin B2. Studies are currently ongoing in our group to further investigate and improve the stabilities and safeties of the avermectin B2 microcapsule preparations with the aim of obtaining microcapsules suitable for use in field applications.

4. MATERIALS AND METHODS

4.1. Materials. Technical avermectin B2 (95%) was purchased from Qilu Pharmaceutical Co., Ltd. (China). Commercial avermectin B2 emulsifiable concentrate (5 wt %) was purchased from Shouguang, Shandong (China). The polymerized isocyanate (MDI, 30% NCO content) was obtained from Wanhua Chemical Group Co., Ltd. (China), while TEOA was purchased from Tianjin Yongda Chemical Reagent Co., Ltd. (China). The fatty alcohol polyoxyethylene polyoxypropylene ether (500#) emulsifier was purchased from Jiangsu Xinde Biological Technology Co., Ltd. (China), while the dispersant (Agrilan 700) and the defoaming agent (SAG*1522) were provided by Nanjing Jierun Technology Co., Ltd. (China). N-Methyl-2-pyrrolidone (NMP, analytical reagent) and glacial acetic acid (analytical reagent) were purchased from Sinopharm Chemical Reagent Co. (Beijing, China). HPLC-grade methanol and acetonitrile were purchased from Thermo Fisher Scientific Inc. (USA). Purified water (Wahaha, China) was used for all reactions and treatment processes. All other chemicals were of analytical grade and were used without further purification.

4.2. Microcapsules Preparation. As outlined in Figure 10, MDI and TEOA were polymerized at the interface of an oil-in-water (O/W) emulsion to prepare the avermectin B2 microcapsules. More specifically, Agrilan 700 (3.0 g) was dissolved in purified water (30 g), and SAG*1522 (1.0 g) was added, giving the water phase. In addition, avermectin B2 (5.0

g), 500# (2.5 g), and MDI (5.0 g) were dissolved in NMP to give the oil phase. Subsequently, the oil phase was poured into the water phase and dispersed into small uniform droplets under vigorous stirring. The resulting emulsion was transferred to a three-necked flask and mechanically stirred at 300 rpm, during which time the aqueous TEOA solution (2.0 g, 25 wt %) was added at a uniform rate over 3 min. The interfacial polymerization reaction was then carried out at 50 °C for 2 h to give a suspension of the avermectin B2-containing microcapsules. Finally, the avermectin B2 microcapsules were collected by centrifugation at 4000 rpm and were subsequently freeze-dried at −80 °C for 12 h (FD-1A-80, Shanghai Lan Yi Industrial Co., Ltd., China) (Figure 10).

4.3. Characterization. *4.3.1. Particle Size Analysis.* A laser particle size meter (Bettersize2600, Dandong Baxter Instrument Co., Ltd., China) was used to determine the size distribution of the prepared microcapsules. The D_{10}, D_{50}, and D_{90} values of the microcapsules were also determined; these values represent the corresponding particle sizes when the cumulative particle size distribution reaches 10, 50, and 90%, respectively, and they are used to evaluate the size distribution range of the microcapsules. It should be noted here that the D_{50} value is commonly used to represent the average size of a microcapsule sample.

4.3.2. Measurement of the Encapsulation Efficiency (EE). The microsphere suspension was dispersed in acetonitrile (10 mL). The resulting mixture was then subjected to centrifugation, and the supernatant was analyzed using high-performance liquid chromatography (HPLC, Agilent 1260, USA) with UV detection. The HPLC separation of avermectin B2 was carried out on an EcoPak 120 C18 column (150 mm × 4.6 mm, 5 μm, Nano Chromechnology Co., Ltd.), with the isocratic elution of methanol/acetonitrile/water (40:40:20, v/

v/v) as the mobile phase. The analyte (10 μL) was injected into the HPLC system and separated at 30 °C, using a constant flow rate of 1.0 mL min^{-1} at a detection wavelength of 245 nm.[36] The retention time of avermectin B2 was approximately 12.7 min. The EE was calculated according to eq 1 as follows

$$EE(\%) = \frac{\text{mass avermectin B2 microcapsules}}{\text{initial mass of avermectin B2}} \times 100 \quad (1)$$

4.3.3. Scanning Electron Microscopy (SEM).
A high- and low-vacuum scanning electron microscope (JSM-6360LV, Jel Ltd, Japan) was used to characterize the morphologies and structures of the avermectin B2 microcapsules.

4.3.4. Fourier Transform Infrared (FTIR) Spectroscopy.
A mixture of the solid sample was mixed with KBr powder and pressed to form a disk. The FTIR spectra of the samples were recorded using a Thermo-Nicolet Nexus 410 FTIR spectrometer (Nibco Colliers Instrument Company, USA) over a wavelength range of 4000−450 cm^{-1}.

4.3.5. Thermodynamic Properties of the Avermectin B2 Microcapsules.
An integrated TGA instrument (TGA-103, Beijing JinYang Wanda Technology Co., Ltd. China) was used for thermal stability analysis of dried samples of the avermectin B2 microcapsules. The measurement conditions were as follows: temperature increase from 25 to 750 °C at a rate of 10 °C min^{-1} and then natural cooling to 25 °C. All measurements were carried out under a 20 mL min^{-1} flow of nitrogen gas.

4.4. Release Rate of Avermectin B2 from the Pesticide-Loaded Microcapsules.
The release kinetics of avermectin B2 from the microcapsules were studied using the dialysis bag method. More specifically, the avermectin B2 microcapsule suspension (1.0 g) was added to a dialysis bag (size: 6 cm, Mw: 8000−14,000), which was sealed and placed in a flask containing the release medium (50 mL, 50 vol% aqueous methanol, v/v). The release test was carried out at 25 °C and 200 rpm in a double-layer thermostatic oscillator (HZQ-F160, Suzhou Peiying Experimental Equipment Co., Ltd., China). Aliquots (1.0 mL) of the medium outside the dialysis bag were collected at different time intervals, and a portion of freshly prepared 50% aqueous methanol (1.0 mL) was added to supplement the removed liquid. The collected samples were stored in a refrigerator (BCD-216SDN, Qingdao Haier Co., Ltd, China) prior to HPLC analysis. As described previously,[37] the cumulative amount of the released avermectin B2 was calculated according to eq 2

$$m_{t-\text{act}} = \left(c_t + \frac{v}{V}\sum_{0}^{t-1} c_t\right) \times v \quad (2)$$

where $m_{t-\text{act}}$ represents the cumulative release amount of avermectin B2 at time t, C_t represents the concentration of avermectin B2 in the release medium at time t, V represents the volume of the release medium removed at each time point (1.0 mL), and V is the total volume of the release medium (50 mL). The release curve was plotted according to the release time and the cumulative release amount, and the release model was used to fit the curve. More specifically, the cumulative release curves of the microcapsules were fitted using the following mathematical models:

(1) The zero-order release model[38]

$$Q_t = Q_0 + k_0 t \quad (3)$$

where Q_t is the amount of active ingredient released at time t, Q_0 is the amount of the active ingredient in the release medium, and k_0 is the release constant;

(2) The first-order release model[39]

$$\text{Ln } Q_t = \text{Ln } Q_0 + k_1 t \quad (4)$$

where Q_t is the amount of active ingredient released at time t, Q_0 is the initial amount of the active ingredient in the microcapsule sample, and k_1 is the release constant;

(3) The Higuchi release model[40]

$$Q_t = Q_0 + k_H t^{1/2} \quad (5)$$

where Q_t is the amount of active ingredient released at time t, Q_0 is the amount of the active ingredient in the release medium, and k_H is the release constant; and

(4) The Ritger−Peppas model[41]

$$Q_t = kt^n \quad (6)$$

where Q_t is the released amount of active ingredient at time t, k is the release constant, and n is the kinetic parameter.

4.5. Photodegradation Studies.
Identical masses of avermectin B2 microcapsules and technical avermectin B2 were placed in Petri dishes and incubated under natural light conditions for 192 h to study their photolytic effects. Samples (20 mg) were removed at different intervals, dissolved in methanol (25 mL), and analyzed by HPLC to detect any changes in the avermectin B2 content.[42]

4.6. Soil Leaching Test.
The soil leaching characteristics of different avermectin B2 preparations were determined using a soil column leaching test. More specifically, the test soil (720 g) was weighed through a 20-mesh sieve and used to fill a cylindrical PVC plastic tube (5 cm × 35 cm) to give a soil column measuring approximately 30 cm. The surface layer of the soil column was paved with quartz sand (1.0 cm thickness) and saturated with a 0.1 mol L^{-1} CaCl$_2$ solution.[43] Subsequently, an aliquot (1.0 mL) of the desired avermectin B2 solution preparation (10 mg/mL) was evenly added dropwise onto the quartz sand layer and leached with a 0.01 mol/L CaCl$_2$ solution at a rate of 30 mL/h; a total of 300 mL of the leaching solution was collected. After leaching, the soil column was evenly divided into six sections, and the avermectin B2 contents in the various sections of the soil and in the leaching solution were measured. All treatments were repeated in triplicate.

4.7. Laboratory Biological Activity Determination.
The laboratory bioactivity test employed cucumber seedlings as the experimental crops, while the second instar larvae of root-knotted nematodes (*Meloidogyne incogntta*), which were sensitive strains reared in the laboratory, were selected as the test targets. Potted root irrigation sandy soil and loam were mixed in a ratio of 2:1 and sterilized. When the cucumber seedlings had produced a single leaf, they were transplanted into a sterilized sandy loam. The avermectin B2 microcapsules and technical avermectin B2 were configured at four concentrations of 0.625, 1.25, 2.5, and 5 mg/L. After transplanting the seedlings, the configured avermectin microcapsule suspension and technical avermectin B2 were used for irrigation purposes (30 mL per plant). In addition, water (30 mL) was used as a blank control. At the same time, a spherical hole measuring approximately 4 cm in depth and 1 cm in diameter was introduced around the seedling using a wooden

stick, and the nematode suspension was used to inoculate the cucumber roots (2000 heads per treatment).[44] A total of 20 seedlings were treated in each group, and each group of experiments was repeated three times. The treated samples were placed in an incubator, and the intact roots were removed after 15 d. After washing with clean water, the number of root nodes was evaluated. The test method is described in GB/T 13917.1−2009 (China).[46]

The regression equation, EC_{50} value (i.e., the effective concentration required to cause inhibition by 50%), and 95% confidence limit were obtained for each tested agent using DPS data processing software for statistical analysis.[45] The indoor toxicity of the tested agent was evaluated according to the EC_{50} value, and the significance of the differences among the samples was statistically analyzed.

4.8. Field Efficacy Test. The field efficacy test was conducted in the tomato sheds of Lingbei Village, Hongshan Sub-district Office, Lingyuan, Liaoning Province. The test field consisted of smooth and sandy loam soil, with ridges measuring 4.4 m in length by 1.3 m in width. These ridges were rich in organic matter and were subjected to normal fertilization and water management. The occurrence of root-knot nematodes was known to be severe in this area in recent years, and no other pesticides had been used in the test field. The effects of the commercial avermectin B2 EC (225 and 375 g ai/hm^2) and the avermectin B2 microcapsule suspensions (225 and 375 g ai/hm^2) on nematode root node control were compared. Each treatment was carried out in triplicate. The control effect was calculated by counting the number of root knots. The investigation method, classification, and pharmacodynamic calculations were as those described in GB/T 17980.38−2000 (China).[47]

$$\text{control effect}(\%) = \frac{a - b}{a} \times 100 \tag{7}$$

where a is the number of blank control group root knots and b is the number of root knots in the evaluation specimen.

AUTHOR INFORMATION

Corresponding Author

Liying Wang − *Institute of Functional Molecules, Shenyang University of Chemical Technology, Shenyang 110142, China;* orcid.org/0000-0003-3422-7409; Email: wangliying401@163.com

Authors

Xinxin Yan − *Institute of Functional Molecules, Shenyang University of Chemical Technology, Shenyang 110142, China*

Yan Li − *Institute of Functional Molecules, Shenyang University of Chemical Technology, Shenyang 110142, China*

Chong Gao − *Institute of Functional Molecules, Shenyang University of Chemical Technology, Shenyang 110142, China*

Junzhi Liu − *Institute of Functional Molecules, Shenyang University of Chemical Technology, Shenyang 110142, China*

Complete contact information is available at:
https://pubs.acs.org/10.1021/acsomega.3c00244

Notes
The authors declare no competing financial interest.

ACKNOWLEDGMENTS

REFERENCES

(1) Eloh, K.; Sasanelli, N.; Maxia, A.; Caboni, P. Untargeted metabolomics of tomato plants after root-knot nematode infestation. *J. Agric. Food Chem.* **2016**, *64*, 5963−5968.

(2) Forghani, F.; Hajihassani, A. Recent Advances in the Development of Environmentally Benign Treatments to Control Root-Knot Nematodes. *Front. Plant. Sci.* **2020**, *11*, 1125.

(3) Reynolds, A. M.; Dutta, T. K.; Curtis, R. H.; Powers, S. J.; Gaur, H. S.; Kerry, B. R. Chemotaxis can take plant-parasitic nematodes to the source of a chemo-attractant via the shortest possible routes. *J. R. Soc. Interface* **2011**, *8*, 568−577.

(4) Krif, G.; Lahlali, R.; El Aissami, A.; Laasli, S.-E.; Mimouni, A.; Serderidis, S.; Picaud, T.; Moens, A.; Dababat, A. A.; Fahad, K.; Mokrini, F. Efficacy of authentic bio-nematicides against the root-knot nematode, Meloidogyne javanica infecting tomato under greenhouse conditions. *Physiol. Mol. Plant Pathol.* **2022**, *118*, No. 101803.

(5) Jing, T.-f.; Zhang, D.-x.; Pan, S.-h.; Liu, G.; Mu, W.; Hou, Y.; Liu, F. Phenyl isocyanate-modified avermectin b1a improves the efficacy against plant-parasitic nematode diseases by facilitating its soil mobility. *ACS Sustainable Chem. Eng.* **2020**, *8*, 2310−2319.

(6) Mrozik, H.; Eskola, P.; Linn, B.; Lusi, A.; Shih, T.; Tischler, M.; Waksmunski, F.; Wyvratt, M.; Hilton, N.; Anderson, T.; et al. Discovery of novel avermectins with unprecedented insecticidal activity. *Experientia* **1989**, *45*, 315−316.

(7) Wang, M.; Yang, X.-H.; Wang, J.-D.; Wang, X.-J.; Chen, Z.-J.; Xiang, W.-S. New β-class milbemycin compound from Streptomyces avermitilis NEAU1069: fermentation, isolation and structure elucidation. *J. Antibiot.* **2009**, *62*, 587−591.

(8) Xu, Q.; Li, J.; Guo, W.; Xiang, J.; Zhou, L.; Zhang, J. High Value Utilization of an Avermectin Fermentation Byproduct: Novel B2a Derivatives as Pesticide Candidates. *J. Agric. Food Chem.* **2022**, *70*, 6377−6384.

(9) Campbell, W. C. History of avermectin and ivermectin, with notes on the history of other macrocyclic lactone antiparasitic agents. *Curr. Pharm. Biotechnol.* **2012**, *13*, 853−865.

(10) Bertozzi, C. R. Chemistry Is Central to Repairing Genes and Global Health: Reflections on the 2015 Nobel Prizes in Chemistry and Physiology or Medicine. *ACS Cent. Sci.* **2015**, *1*, 343−344.

(11) Jones, J. T.; Haegeman, A.; Danchin, E. G.; Gaur, H. S.; Helder, J.; Jones, M. G.; Kikuchi, T.; Manzanilla-López, R.; Palomares-Rius, J. E.; Wesemael, W. M.; Perry, R. N. Top 10 plant-parasitic nematodes in molecular plant pathology. *Mol. Plant Pathol.* **2013**, *14*, 946−961.

(12) Quentin, M.; Abad, P.; Favery, B. Plant parasitic nematode effectors target host defense and nuclear functions to establish feeding cells. *Front. Plant Sci.* **2013**, *4*, 53.

(13) Su, C.; Ji, Y.; Liu, S.; Gao, S.; Cao, S.; Xu, X.; Zhou, C.; Liu, Y. Fluorescence-labeled abamectin nanopesticide for comprehensive control of pinewood nematode and Monochamus alternatus Hope. *ACS Sustainable Chem. Eng.* **2020**, *8*, 16555−16564.

(14) Chin, C.-P.; Lan, C.-W.; Wu, H.-S. Application of biodiesel as carrier for insecticide emulsifiable concentrate formulation. *J. Taiwan Inst. Chem. Eng.* **2012**, *43*, 578−584.

(15) Hung, W. H.; Chen, P. K.; Fang, C. W.; Lin, Y. C.; Wu, P. C. Preparation and Evaluation of Azelaic Acid Topical Microemulsion Formulation: In Vitro and In Vivo Study. *Pharmaceutics* **2021**, *13*, 410.

(16) He, R.; Wang, J.; Wang, X.; Li, W.; Zhang, X. Fabrication and characterization of core−shell novel PU microcapsule using TDI trimer for release system. *Colloids Surf. A* **2018**, *550*, 138−144.

(17) Xu, Y.; Chen, W.; Guo, X.; Tong, Y.; Fan, T.; Gao, H.; Wu, X. Preparation and characterization of single-and double-shelled

cyhalothrin microcapsules based on the copolymer matrix of silica−N-isopropyl acrylamide−bis-acrylamide. *RSC Adv.* **2015**, *5*, 52866−52873.

(18) Wang, X.; Yin, H.; Chen, Z.; Xia, L. Epoxy resin/ethyl cellulose microcapsules prepared by solvent evaporation for repairing microcracks: Particle properties and slow-release performance. *Mater. Today Commun.* **2020**, *22*, No. 100854.

(19) Ke, W.-D.; Wu, X.-W.; Zhang, J.-L. In situ polymerization of organic and inorganic phase change microcapsule and enhancement of infrared stealth via nano iron. *Colloids Surf. A* **2021**, *627*, No. 127124.

(20) Zhou, Y.; Cui, Y.; Wang, X.; Zhang, M.; Zhang, M.; Gao, Y.; Gao, Y.; Wang, H. Melamine-formaldehyde microcapsules encapsulating HEDP for sustained scale inhibition. *Colloids Surf. A* **2021**, *628*, No. 127361.

(21) Yamazaki, T.; Ogawa, A.; Koizumi, H.; Tsuji, T. Controlled soap-free emulsion polymerization stability using a novel cationic azo radical initiator with chloride or triflate counter anion. *Colloids Surf. A* **2021**, *609*, No. 125614.

(22) Xu, D.; Yang, R. Efficient preparation and characterization of paraffin-based microcapsules by emulsion polymerization. *J. Appl. Polym. Sci.* **2019**, *136*, 47552.

(23) Qin, Y.; Lu, X.; Que, H.; Wang, D.; He, T.; Liang, D.; Liu, X.; Chen, J.; Ding, C.; Xiu, P.; Xu, C.; Gu, X. Preparation and Characterization of Pendimethalin Microcapsules Based on Microfluidic Technology. *ACS Omega* **2021**, *6*, 34160−34172.

(24) Chen, M.; Liu, J.; Liu, Y.; Guo, C.; Yang, Z.; Wu, H. Preparation and characterization of alginate-N-2-hydroxypropyl trimethyl ammonium chloride chitosan microcapsules loaded with patchouli oil. *RSC Adv.* **2015**, *5*, 14522−14530.

(25) Paik, S. U. Environmentally friendly polyurea microcapsules of pesticides by PVA mediated interfacial polymerization. *Mater. Sci. Forum* **2006**, *510−511*, 678−681.

(26) Cao, H.; Chen, Y.; Zhang, D.; Jin, Y.; Zhang, P.; Li, B.; Mu, W.; Liu, F. Octaphenyl polyoxyethylene regulates the flexibility of pyraclostrobin-loaded soft microcapsules by interfacial polymerization for better foliar adhesion and pesticide utilization. *Chem. Eng. J* **2022**, *439*, No. 135805.

(27) Antony, M. J.; Jolly, C. A.; Das, K. R.; Swathy, T. Normal and reverse AOT micelles assisted interfacial polymerization for polyaniline nanostructures. *Colloids Surf. A* **2019**, *578*, No. 123627.

(28) Das, A.; Mahanwar, P. A brief discussion on advances in polyurethane applications. *Adv. Ind. Eng. Polym. Res.* **2020**, *3*, 93−101.

(29) Mahajan, N.; Gupta, P. New insights into the microbial degradation of polyurethanes. *RSC Adv.* **2015**, *5*, 41839−41854.

(30) Yu, F.; Wang, Y.; Zhao, Y.; Chou, J.; Li, X. Preparation of polyurea microcapsules by interfacial polymerization of isocyanate and chitosan oligosaccharide. *Materials* **2021**, *14*, 3753.

(31) Zhao, L.; Yang, X.; Ma, L.; Li, Q. Preparation of imidazole embedded polyurea microcapsule for latent curing agent. *J. Appl. Polym. Sci.* **2020**, *137*, 49340.

(32) Zheng, T.; Chen, K.; Chen, W.; Wu, B.; Sheng, Y.; Xiao, Y. Preparation and characterisation of polylactic acid modified polyurethane microcapsules for controlled-release of chlorpyrifos. *J. Microencapsul.* **2019**, *36*, 62−71.

(33) Fu, Y.; He, H.; Liu, R.; Zhu, L.; Xia, Y.; Qiu, J. Preparation and performance of a BTDA-modified polyurea microcapsule for encapsulating avermectin. *Colloids Surf. B* **2019**, *183*, No. 110400.

(34) Katagi, T. Soil Column Leaching of Pesticides. In *Reviews of Environmental Contamination and Toxicology*, 2013; Vol. *221*, pp 1−105.

(35) Kalyabina, V. P.; Esimbekova, E. N.; Kopylova, K. V.; Kratasyuk, V. A. Pesticides: Formulants, distribution pathways and effects on human health − A review. *Toxicol. Rep.* **2021**, *8*, 1179−1192.

(36) Jahromi, A. K.; Shieh, H.; Saadatmand, M. Theoretical study of diffusional release of a dispersed solute from cylindrical polymeric matrix: a novel configuration for providing zero-order release profile. *Appl. Math. Model.* **2019**, *73*, 136−145.

(37) Luo, C.; Yang, Q.; Lin, X.; Qi, C.; Li, G. Preparation and drug release property of tanshinone IIA loaded chitosan-montmorillonite microspheres. *Int. J. Biol. Macromol.* **2019**, *125*, 721−729.

(38) Tan, S.; Zhong, C.; Langrish, T. Pre-gelation assisted spray drying of whey protein isolates (WPI) for microencapsulation and controlled release. *LWT* **2020**, *117*, No. 108625.

(39) Dukhin, S. S.; Labib, M. E. Theory of effective drug release from medical implants based on the Higuchi model and physico-chemical hydrodynamics. *Colloids Surf. A* **2012**, *409*, 10−20.

(40) Li, G.-B.; Wang, J.; Kong, X.-P. Coprecipitation-based synchronous pesticide encapsulation with chitosan for controlled spinosad release. *Carbohydr. Polym.* **2020**, *249*, No. 116865.

(41) Feng, J.; Yang, J.; Shen, Y.; Deng, W.; Chen, W.; Ma, Y.; Chen, Z.; Dong, S. Mesoporous silica nanoparticles prepared via a one-pot method for controlled release of abamectin: Properties and applications. *Microporous Mesoporous Mater.* **2021**, *311*, No. 110688.

(42) Deng, Y.; Zhao, H.; Qian, Y.; Lü, L.; Wang, B.; Qiu, X. Hollow lignin azo colloids encapsulated avermectin with high anti-photolysis and controlled release performance. *Ind. Crops Prod.* **2016**, *87*, 191−197.

(43) Eun, H.; Choi, G.; Choi, D.-S.; Hong, S.-M. Performance Evaluation for Endosulfan Removal by Carbon-based Adsorbents. *J. Pestic. Sci.* **2021**, *25*, 111−118.

(44) Shilpa; Sharma, P.; Thakur, V.; Sharma, A.; Rana, R.; Kumar, P. A status-quo review on management of root knot nematode in tomato. *J. Hortic. Sci. Biotech.* **2022**, *97*, 403−416.

(45) Li, J. L.; Liu, X. Y.; Xie, J. T.; Di, Y. L.; Zhu, F. X. A comparison of different estimation methods for fungicide EC50 and EC95 values. *J. Phytopathology* **2015**, *163*, 239−244.

(46) Tao, L.; Wang, X.; Zhang, J.; Xin, Z.; Ji, L.; Huang, Q.; Wu, S. Laboratory efficacy test methods and criterions of public health insecticides for pesticide registration−Part 1:Spray fluid. Standards Press of China: Beijing, 2009.

(47) Wu, X.; Gu, B.; Liu, N.; Zhu, Q. *Pesticide—Guidelines for the Field Efficacy Trials*; Standards Press of China: Beijing, 2000.